



**HAL**  
open science

# A one dimensional, electrostatic Vlasov model for the generation of suprathermal electron tails in solar wind conditions

Francesco Califano, André Mangeney

► **To cite this version:**

Francesco Califano, André Mangeney. A one dimensional, electrostatic Vlasov model for the generation of suprathermal electron tails in solar wind conditions. *Journal of Geophysical Research Space Physics*, 2008, 113 (A06103), pp.6103. 10.1029/2007JA012841 . hal-03732427

**HAL Id: hal-03732427**

**<https://hal.science/hal-03732427>**

Submitted on 25 Aug 2022

**HAL** is a multi-disciplinary open access archive for the deposit and dissemination of scientific research documents, whether they are published or not. The documents may come from teaching and research institutions in France or abroad, or from public or private research centers.

L'archive ouverte pluridisciplinaire **HAL**, est destinée au dépôt et à la diffusion de documents scientifiques de niveau recherche, publiés ou non, émanant des établissements d'enseignement et de recherche français ou étrangers, des laboratoires publics ou privés.

Copyright

## A one dimensional, electrostatic Vlasov model for the generation of suprathermal electron tails in solar wind conditions

F. Califano<sup>1,2</sup> and A. Mangeney<sup>2</sup>

Received 27 September 2007; revised 10 January 2008; accepted 20 February 2008; published 12 June 2008.

[1] Space and laboratory collisionless plasmas are most often out of local thermodynamic equilibrium. In particular, their charged particle velocity distributions usually differ from simple Maxwellian distributions and exhibit a great variety of anisotropies and components such as suprathermal beams and tails. Here we propose a new model responsible for a “local” origin of electron suprathermal tails. The model is based on adding a high and a low frequency external forcing to the Vlasov-Poisson system of equations. The first one represents mainly the thermal noise electric field generated by charge separation effects. The second one represents the energy injection resulting from the energy cascade generated by the large scale fluid (MHD) turbulence. We find that in typical solar wind conditions, our model could be the base of a full three dimensional, electromagnetic model capable of explaining the local generation of the electron halo population observed on the electron distribution function.

**Citation:** Califano, F., and A. Mangeney (2008), A one dimensional, electrostatic Vlasov model for the generation of suprathermal electron tails in solar wind conditions, *J. Geophys. Res.*, 113, A06103, doi:10.1029/2007JA012841.

### 1. Introduction

[2] Space and laboratory collisionless plasmas are most often out of local thermodynamic equilibrium. In particular, their charged particle velocity distributions usually differ from simple Maxwellian distributions and exhibit a great variety of anisotropies and components such as suprathermal beams and tails [see *Christon et al.*, 1989; *Collier*, 1999; *Maksimovic et al.*, 2005] which have been a rich source of problems for space physics research.

[3] This is the case for the electron distribution function in the solar wind which displays both beam like and tail components. Indeed, the electron distribution function in the range of energies less than  $\leq 2$  keV in the solar wind is typically observed to consist of at least three components. The main component is a roughly isotropic, Maxwellian “core” with density  $n_c \sim 10\text{--}40 \text{ cm}^{-3}$  and mean temperature  $T_c \sim 10$  eV. The second component is a diffuse, roughly isotropic halo with density  $n_h \sim 0.01\text{--}0.03 N_c$  which appears at energies greater than  $\sim 60$  eV with an equivalent temperature  $T_h \sim 7\text{--}8T_c$ . The third component consists of a beam like population, the “strahl” which is superposed on the halo and flows along the local magnetic field, with densities  $n_{\text{strahl}}$  comparable to but usually smaller than  $n_h$  streaming away from the sun and carrying an electron heat flux which is an important channel for energy transport in the solar wind [e.g., *Feldman et al.*, 1998].

[4] There is as yet no generally accepted theoretical model which explains these observations. In particular,

one does not have an unambiguous answer to the basic question of whether these suprathermal tails are generated in the solar wind or whether they originate in the solar corona.

[5] The standard interpretation is that the core electron population is collisional and bound by the interplanetary electrostatic potential, its properties being regulated locally. The “strahl” electrons instead are thought to be coronal electrons having velocities large enough to escape without colliding with the background plasma; their temperature is indeed close to the electron temperature in the corona  $\sim 150$  eV. Furthermore suprathermal electrons escaping from the corona and propagating away from the sun along the magnetic field conserve their magnetic adiabatic invariant in a decreasing magnetic field [*Olbert*, 1983], so that their velocity should tend to align with the local magnetic field. This is in contradiction with the *Ulysses* observations by *Hammond et al.* [1996], who found instead that the strahl width broadens substantially between 1.3 and 2.3 AU, indicating the existence of an efficient scattering mechanism. Coulomb collisions can be invoked but their efficiency decreases with the plasma density and the energy of the electrons [*Fairfield and Scudder*, 1985]; the observed rapid decrease in strahl beam size with increasing energy is strikingly similar to the decrease in the collision age (i.e., the number of collisions suffered by a particle during its travel from the sun to the point of observation) related to the strong velocity dependence of the electron mean free path, as noted by *Ogilvie et al.* [2000]. When the density of the solar wind plasma is sufficiently small, as in the high speed wind, coulomb collisions for strahl electrons are almost completely suppressed, and they form a strong anisotropic component in the halo, with a small angular width and an amplitude which varies with the solar wind plasma density [*Ogilvie et al.*, 2000].

<sup>1</sup>Dipartimento di Fisica, Università di Pisa, Pisa, Italy.

<sup>2</sup>LESIA, Observatoire de Paris-Meudon, Meudon, France.

[6] In this scenario, the halo result from the scattering of strahl electrons over spatial length of the order of many AU [Scudder and Olbert, 1979a, 1979b; Saito and Gary, 2007]. As one could expect from a very weakly collisional population, the suprathermal electron component displays a high degree of variability: the halo density  $n_h$ , the angular width and intensity of the strahl electrons all vary widely.

[7] An anticorrelation between  $n_e$  and total  $T_e$  is well known, and has been interpreted as either as being due to pressure balance [Gosling, 1999] or to different collisional histories of the plasma [Hammond et al., 1996]. Phillips and Gosling [1990] demonstrated theoretically that when the density is high, electrons are both more isotropic and cooler. Since the core population is more collisional than the halo we would expect it to be more cooled than the halo in the high density periods. Indeed, the temperature gradients of the core and halo populations are all flatter than the  $R^{-4/3}$  law expected for the adiabatic expansion of an isotropic distribution. The core temperature  $T_c$  has a radial gradient intermediate between isothermal and adiabatic, with the steeper gradients for denser winds. The gradient of the halo temperature  $T_h$  has a similar density dependence, but is much smaller.

[8] Moreover, Maksimovic et al. [2005] in a recent study of the radial evolution of the electron distribution functions in the fast solar wind between 0.3 and 1.5 AU (using data from Helios, Ulysses and Wind) have shown that  $n_h/n_e$  increases while  $n_{\text{strahl}}/n_e$  decreased as the distance from the sun increases as one would expect if the halo electrons result from the diffusion of strahl electrons.

[9] Several studies using various forms of the collision operator (Coulomb collisions) appear also to support partially this picture from the theoretical point of view (see for example, Lie-Svendsen et al. [1997], Lie-Svendsen and Leer [2000], and Pierrard et al. [2001]) by suggesting that this mechanism may diffuse a significant proportion of the strahl electrons and even populate the sunward directed part of the halo.

[10] Other models, based on the quasilinear interactions of the electrons and a suprathermal level of plasma waves or whistler waves, have also been developed; indeed it was shown by Hasegawa et al. [1985] that a nonthermal level of waves can enhance velocity diffusion so as to produce a power law distribution. Ma and Summers [1999], Leubner [2001], and Vocks and Mann [2003] applied these models in the solar wind context.

[11] However, some observations are not easily explained within this scenario. First,  $n_{\text{strahl}}/n_e$  is at most comparable to, but usually smaller than  $n_h/n_e$  at 0.3 AU [Maksimovic et al., 2005] what does not seem to be compatible with the hypothesis that halo electrons are an increasing scattered part of the strahl electrons.

[12] Second, if the halo electrons result from the Coulomb diffusion of strahl electrons, one should observe a very weak halo component when the background electron density decreases as is observed in the high speed wind. This is contrary to the observations by Maksimovic et al. [1997] who fitted the electron distribution functions (as measured by the Ulysses spacecraft) averaged over all directions (thereby eliminating the strahl component) with Kappa distribution functions; they observed that the importance of suprathermal tails i.e.,  $\alpha = n_h/n_c$  was higher in fast

solar winds than in the slow wind. They suggested that this observation supported kinetic exospheric theories of the solar wind expansion since, in this model, an increased number of escaping coronal electrons is associated with a faster solar wind flow. However, such an argument should apply only to the strahl electrons and not to the isotropic halo.

[13] Third, globally,  $\alpha = n_h/n_c$  and  $n_e = n_c + n_h$  are anticorrelated while  $T_c$  and  $T_h$  do not seem to depend on  $n_e$  [Skoug et al., 2000]. Skoug et al. [2000] interpreted this anticorrelation as a consequence of a statistical independence between  $n_c$  and  $n_h$ , what seems to be hard to understand if the halo electrons result from the scattering of the strahl electrons on the core electrons.

[14] A local origin of electron suprathermal tails has also been proposed by Vinas et al. [2000] in a different context (in the near solar atmosphere), suggesting that among the low frequency large scale waves expected to be found in the corona, some displayed a strong magnetic field aligned electrostatic component. If such an electrostatic sinusoidal field is used as an initial condition, the Vlasov-Poisson evolution of a one dimensional plasma leads to the excitation of a high level of Langmuir waves and the formation of high energy tails in the electron distribution. However, the initial electric potential energy they used in their simulations was of the order or larger than the average electron kinetic energy. Such large electric fields are not observed in the solar wind and such an interpretation cannot be used in the present context. Recently, a weak turbulence approach has been used involving Langmuir and ion sound waves in the framework of a beam-plasma interaction. It has been shown that self-consistent generation of energetic electron tails by turbulent acceleration is possible only in the presence of some ‘‘collisional’’ effect. In particular, the authors point out that the *spontaneous scattering term*, proportional to the  $g$  plasma parameter, is responsible for the high energy tail generation. Therefore suprathermal electron tails cannot be produced in a purely mean field (Vlasov) approach [Yoon et al., 2006; Rhee et al., 2006].

[15] We shall use as a starting point the observation that the ‘‘quasi-thermal’’ electrostatic noise continuously observed in the solar wind [see Meyer-Vernet and Perche, 1989; Chateau and Meyer-Vernet, 1991] is in equilibrium with the halo electrons, the peak intensity being proportional to  $T_h$ , and we shall investigate under what conditions one can generate locally such an equilibrium between suprathermal electron tails and an enhanced level of plasma oscillations. For this, we make use of two external forcing terms in the standard Vlasov-Poisson system of equations for a collisionless plasma, aiming to model two typical ingredients of collisionless space plasmas (as for example the solar wind) discussed in the following. The first forcing, at high frequencies, models the electric field generated by charge separation due to thermal noise (discretized particles effects). It is a standard way of introducing ‘‘collisions’’ in mean field simulations except that here, for the sake of simplicity, we do not impose self-consistency which means that our forcing is independent of the distribution function. Since the high frequency forcing models an electric field, it is present in both the proton and the electron Vlasov equations.

[16] The second forcing, at low frequencies, is meant to model quasi-neutral, relatively large scale density fluctua-

tions. It appears in the Vlasov proton equation only. Indeed, in the case of a vanishing high frequency forcing, the low frequency force generates only quasi-neutral fluctuations, without any significant charge separation. The origin of the density fluctuations can be thought as to be produced by a non linear cascade generated by the large scale fluid (MHD) turbulence. This kind of effect has been observed in recent Vlasov-hybrid simulations where finite amplitude, large scale Alfvén waves propagating along the mean magnetic field generate density fluctuations with typical wavelengths of the order or less than the ion skin depth (F. Valentini et al., private communications).

[17] Because of the complexity of the full problem, we limit our model to purely electrostatic simulations. The main reason is that at the typical frequencies we are concerned with,  $f > 10$  Hz, cluster observations show that the RMS value of the magnetic fluctuations is smaller than  $10^{-3}$  nT [C. Lacombe et al., private communications]. On the other hand, the RMS value of the electric noise in a solar wind Maxwellian plasma at the core temperature is of the order of  $10^{-1}$  mV/m. Therefore the magnetic term in the Lorentz force is negligible with respect to the “collisional” electric field, while it may play a role in the isotropisation of the super thermal particles [Saito and Gary, 2007].

[18] As a final remark, we note that the solar wind is a weakly magnetized plasma,  $\omega_{ce}/\omega_{pe} \sim 0.1$ , (where  $\omega_{ce}$  and  $\omega_{pe}$  are the electron cyclotron and plasma frequency). However, the collisional time associated to the high frequency forcing is much larger than the electron gyroperiod. Therefore the corresponding “collisional” effects should strongly be affected by the mean magnetic field leading to a strong anisotropy in the magnetic field direction. Since a full 3D, magnetized Vlasov simulation is beyond our computational capabilities, we consider here the 1D electrostatic limit aligned with the magnetic field. One may speculate that the whistler diffusion discussed by Saito and Gary [2007] will help the system to reach a more isotropic situation. Therefore our approach must be considered as a starting point toward a fully three-dimensional, magnetized model.

## 2. Vlasov Equation With Random Forces

[19] Collisionless plasma dynamics is dominated by collective processes when the Debye length  $\lambda_D$  is much greater than the typical interparticle distance ( $\bar{n}$  being a typical density)

$$\lambda_* = \left(\frac{4\pi\bar{n}}{3}\right)^{-1/3}$$

i.e., when  $\lambda_D \gg \lambda_*$ . In the Vlasov description the discrete character of the particles has been lost; the particles advance in an “average” electric field  $\bar{E}$  determined by solving the Poisson equation using the one particle distribution functions,  $f_e(x, v, t)$  and  $f_p(x, v, t)$ ,

$$\frac{\partial \bar{E}}{\partial x} = e \left[ \int f_p(x, v, t) dv - \int f_e(x, v, t) dv \right]$$

However, even at equilibrium when  $\bar{E} = 0$ , it remains a fluctuating electric field  $E_*$  related to the thermal motion of discrete charged particles. The RMS order of magnitude  $E_*$  of this electric noise for a Maxwellian plasma is of the order of the average unscreened electric force between neighboring protons,  $E_* = e/\lambda_*^2$  which, in dimensionless units, ( $\bar{E} = m_e v_{th,e} \omega_{pe} / e$ , see below) becomes

$$E_* \sim n_D^{-1/3} \quad (1)$$

where  $n_D = \bar{n}(4\pi\lambda_D^3/3) \gg 1$ . For typical solar wind parameters,  $n \sim 10 \text{ cm}^{-3}$  and  $\lambda_D = 10^3 \text{ cm}$ , we get  $n_D = 4 \cdot 10^{10}$  and  $E_* \sim 3 \cdot 10^{-4}$ . In dimensional units, the normalizing electric field turns out to be  $\bar{E} \simeq 15 \text{ mV/m}$  and the RMS fluctuating electric field  $\tilde{E}_* \simeq 5 \cdot 10^{-3} \text{ mV/m}$ .

[20] This “thermal” level of electrostatic noise may be much higher if the distribution functions are not Maxwellian. There is a close relationship between these electrostatic fluctuations and Coulomb collisions. In particular, the Lennard Balescu equation, which describes the effects of cumulative “soft” collisions in a plasma,

$$\frac{\partial f}{\partial t} = \frac{\partial}{\partial v} \left[ D(v) \frac{\partial f}{\partial v} - A(v)f \right] \quad (2)$$

can be viewed as the quasilinear diffusion of electrons in this noise field with the diffusion coefficient given by

$$D(v) = \frac{e^2}{m} \int \int d\omega d\mathbf{k} \frac{k_i k_j}{k^2} \langle E^2(\mathbf{k}, \omega) \rangle \delta(\omega - \mathbf{k} \cdot \mathbf{v})$$

and a corresponding expression for the friction coefficient [Alexandrov et al., 1984]. Therefore the interplay of spontaneous emission and absorption of plasma waves by electrons described by equation (2) leads to a relaxation toward local thermal equilibrium, i.e., Maxwellian distribution functions, unless some external forcing is exerted on the plasma. We shall argue that if this external forcing is due to the effects of “low frequency” waves, then the relaxation is toward distribution functions with weakly heated core but with suprathermal tails.

[21] Spontaneous emission as well as the other particle discreteness effects and the corresponding random electrostatic fluctuations are not included in the mean field approximation where the evolution of the particle distribution functions are described by the Vlasov equations. We shall therefore turn to a method similar to that used to model collisions in PIC codes, the so-called “collision field” model [Jones et al., 1996; Mannheimer et al., 1997; Qiang et al., 2000; Albright et al., 2001], where  $e - e$  collision effects are represented as a stochastic motion of a single electron, rather than as a pairwise process. The dynamical and stochastic diffusion coefficients for the Langevin equation can be represented by velocity dependent quantities,

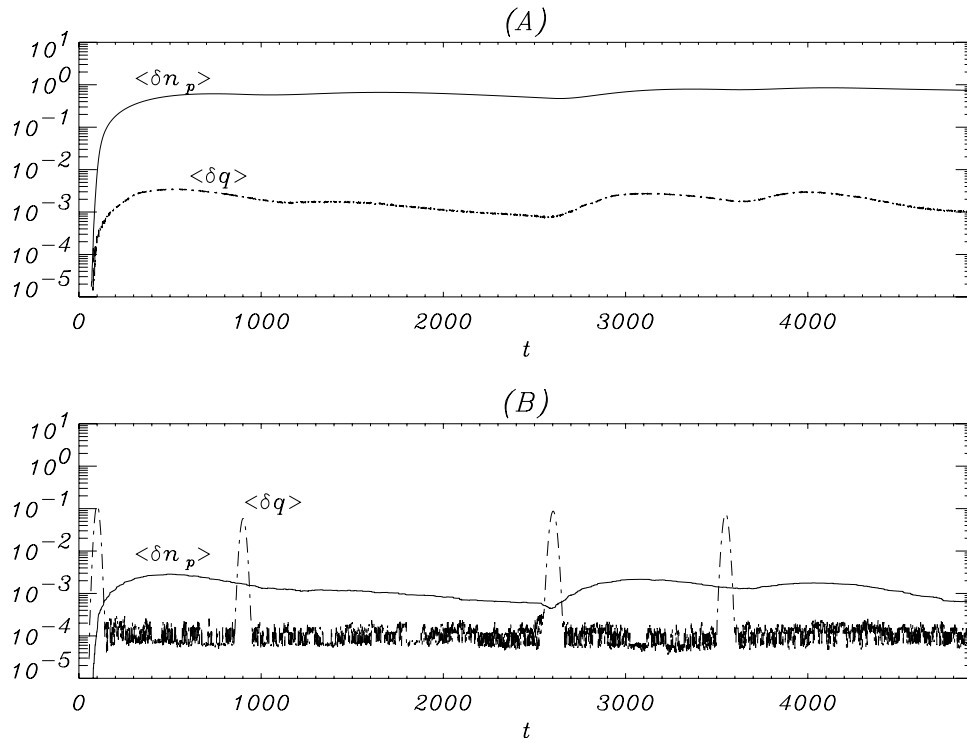


**Figure 1.** (a) Square root of the space averaged squared proton density,  $\langle \delta n_p \rangle$ , and charge fluctuations,  $\langle \delta q \rangle$ , in the presence of a low frequency forcing acting on the protons only. (b) Same as Figure 1a for the same low frequency forcing applied also on the electrons. The square root of the space averaged squared electron density,  $\langle \delta n_e \rangle$ , curve turns out to be superposed to the protons in Figure 1a and to the maximum between the protons and charge fluctuations curve in Figure 1b.

which are simply added to the macroscopic electromagnetic forces acting on the electrons; if the random forces are Markovian, this is a priori fully equivalent to the Fokker-Planck equation (2) describing the effect of long range Coulomb collisions.

[22] The basic set of equations are the stochastic differential equations

$$\frac{dx}{dt} = v(t); \frac{dv}{dt} = -\frac{e}{m} \left( E - \frac{1}{2} \frac{\partial D}{\partial v} \right) + \sqrt{2D} \beta(t)$$

where  $\beta(t)$  is a normally distributed random variable, of unit variance. Such random forces can also be used to describe the effects of collisions in the Vlasov equation; however, existing models do not take into account the plasma screening effect in the interparticle interactions, described by the presence of the dielectric constant in the Lennard Balescu equation. Therefore we have used an oversimplification of the random force, without any attempt to self consistency, by introducing random external electric charges  $\delta q(x, t)$  with given statistical properties in the Poisson equation. The resulting electric field (and its potential) is then the superposition of the self consistent field  $E(x, t)$  (with potential  $\phi$ ) and a random electric field

$E_r(x, t)$  (with potential  $\Psi_{HF}$ ). In dimensionless variables, Poisson's equation may be written as

$$\begin{aligned} \frac{\partial(E + E_r)}{\partial x} &= \left( \int f_p dv - \int f_e dv \right) + \delta q(x, t); \\ E &= -\frac{\partial \phi}{\partial x}; \quad E_r = -\frac{\partial \Psi_{HF}}{\partial x} \end{aligned} \quad (3)$$

### 3. Model

[23] We solve the Vlasov-Poisson system of equations in the  $(x, v)$  phase space for an electrons protons plasma and we add an external high frequency (hereafter HF) forcing modeling (consistently to our “simple” model, equation (3)) the electric field induced by discrete particles effects. We also introduce a low frequency (hereafter LF) forcing in the proton Vlasov equation which models the motions driven, for example, by an energy cascade of the large scale fluid fluctuations. In dimensionless units, the equations read:

$$\frac{\partial f_e}{\partial t} + v \frac{\partial f_e}{\partial x} + (\nabla \phi - \epsilon \nabla \Psi_{HF}) \frac{\partial f_e}{\partial v} = 0 \quad (4)$$

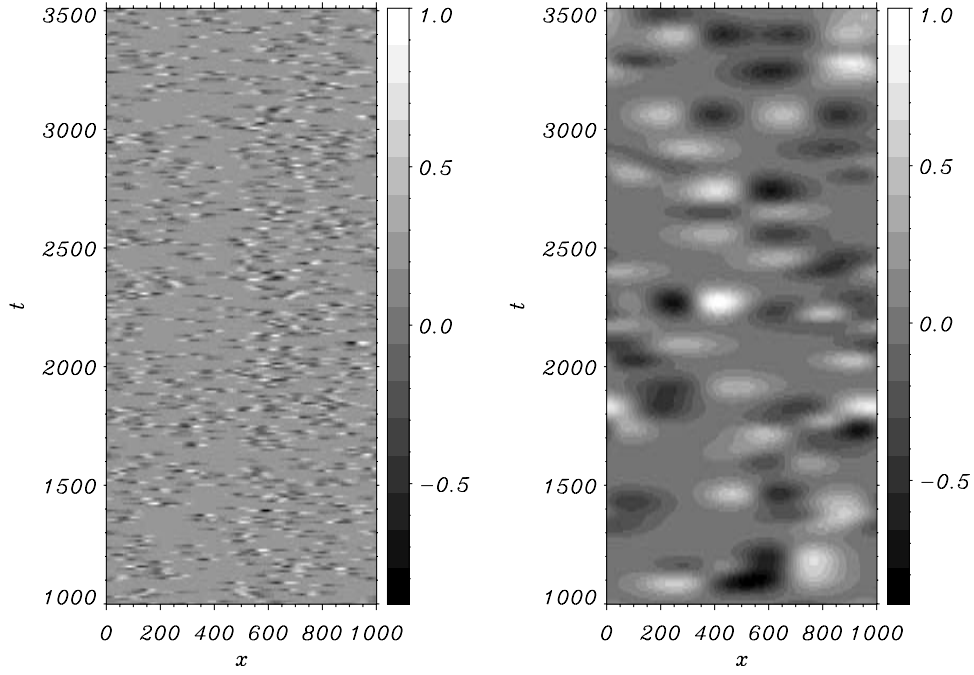


**Figure 2.** HF (left) and LF (right) forcing. The HF forcing is defined in equation (9) with  $N = 1244$ ,  $h_x = 30$ ,  $h_t = 1$ . The LF forcing is defined in equation (7) with  $K = 62$ ,  $\ell_x = 150$ ,  $\ell_t = 50$ .

$$\frac{\partial f_p}{\partial t} + v \frac{\partial f_p}{\partial x} - \frac{m_e}{m_p} (\nabla \phi - \eta \nabla \Psi_{LF} - \epsilon \nabla \Psi_{HF}) \frac{\partial f_p}{\partial v} = 0 \quad (5)$$

$$\nabla^2 \phi = \int f_e dv - \int f_p dv; \quad E = -\nabla \phi \quad (6)$$

These equations are normalized on the following characteristic quantities: the mass of the electron  $m_e$ , the characteristic density  $\bar{n}$ , the electron thermal velocity  $v_{th,e}$ , the Debye length  $\lambda_D$  and the inverse of the plasma frequency  $\omega_{pe}^{-1}$ . The electric field is normalized to  $\bar{E} = m_e v_{th,e} \omega_{pe} / e$ . We use periodic boundary conditions in the interval  $x \in [0, L_x]$ . In all simulations presented here we have taken  $m_e/m_p = 1/1836$ .

[24] In equations (4)–(5)  $\Psi_{LF}$  and  $\Psi_{HF}$  are the potentials of the external forcing varying on a low (proton) and high (electron) timescale,  $\tau_{LF} \sim \sqrt{m_p/m_e}$ , and  $\tau_{HF} \sim 1$ , respectively.

### 3.1. Low Frequency Forcing

[25] The LF forcing term in equation (5) is characterized by a number of space-time Gaussian pulses of the following form:

$$\Psi_{LF} = A_{LF} \sum_{k=1}^K a_n e^{-(x-x_k)^2/\ell_x} e^{-(t-t_k)^2/\ell_t}, \quad (7)$$

where  $A_{LF}$  is a normalization factor such that  $\max(\nabla \Psi_{LF} = 1)$ ,  $a_n \in [-1, 1]$  are random amplitudes,  $K$  is the total number of “events”,  $x_k$  and  $t_k$  the random distributed

positions and  $\ell_x$  and  $\ell_t$  the characteristic length and timescale.

[26] This forcing is characterized by the fact that it drives ballistically several spatial plasma compressions or rarefactions. Despite its simple form, it contains the essential features of more complicated analytical expression, as checked in a number of numerical experiments (not shown here) where the global effect on the plasma of more complicated analytical forms of  $\Psi_{LF}$  can be represented as a sum of plasma compressions and rarefactions on the proton density.

[27] Since the LF forcing term models the long proton timescale motions, we assume that the electrons response is adiabatic, without producing any charge separation:

$$n_e = n_0 e^{e\phi/k_B T_e}; \quad n_e \simeq n_p \quad (8)$$

Such a response of the electrons is well modeled in a Vlasov simulation by inserting the LF forcing term only in the proton equation, equation (5). This is demonstrated by performing two simulations using only the LF forcing term (i.e.,  $\epsilon = 0$  in equations (4)–(6) with  $\eta = 1$ ,  $K = 4$ ,  $\ell_x = 40$ ,  $\ell_t = 25$ ). The only difference between the two runs A and B is that in run B we apply the LF forcing term also on the electron Vlasov equation. In these simulations, the forcing term is characterized by four events ( $K = 4$ ), namely two plasma rarefactions at  $x = 500$  and  $x = 800$  with maximum at  $t_1 = 100$  and  $t_3 = 2600$ , respectively, and two plasma compression at  $x = 200$  and  $x = 700$ , with maximum at  $t_2 = 900$  and  $t_4 = 3550$ , respectively.

[28] The results are summarized in Figure 1 where we plot  $\langle \delta n_p \rangle$  and  $\langle \delta q \rangle$  resulting from run A and B, frames (A)

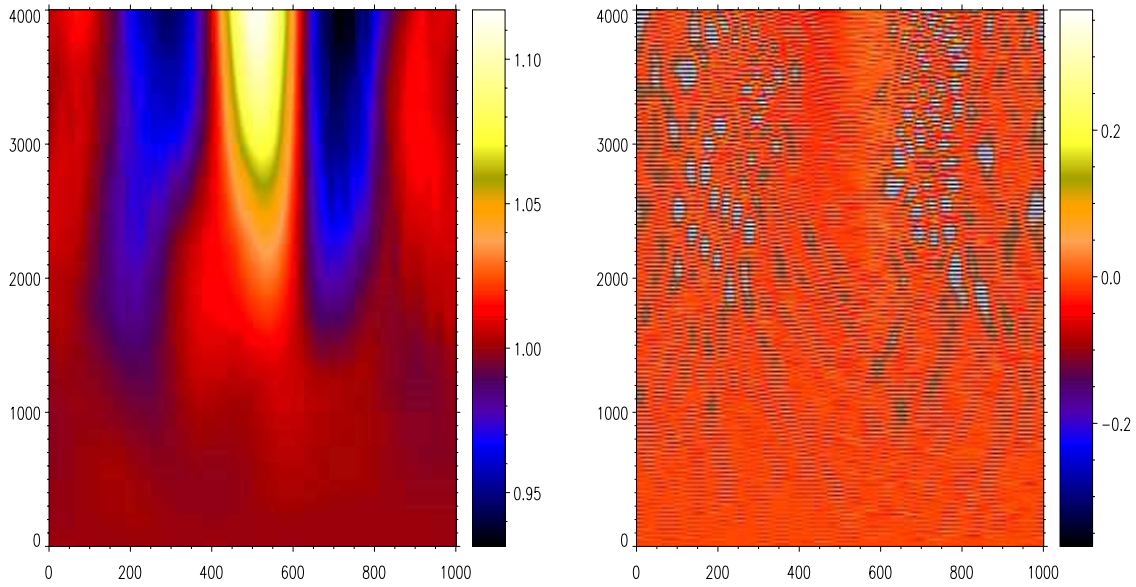


**Figure 3.** Proton density and the electric field in the  $(x, t)$  plane for a simulation with  $\eta = 0.03$  and  $\epsilon = 0.03$ .

and (B), respectively (here  $\delta q = n_p - n_e$  and  $\langle \dots \rangle$  is the square root of the spatial average of the squared fluctuations).

[29] When the LF forcing is applied to the protons only, frame (A), we observe a very low level of charge separation completely uncorrelated with respect to the forcing. The electron density fluctuations follow a Boltzmann distribution, equation (8). On the other hand, when also the electrons are forced by the LF term, frame (B), the response is non adiabatic producing strong charge separation during the (four) forcing events; in this case the electron response is able to screen the LF forcing leading to a much lower protons fluctuations level. In the following, the LF forcing will never be applied to the electrons, as consistent with equation (4) where such term is absent.

### 3.2. High Frequency Forcing

[30] We consider a HF forcing term not completely random, but with a certain degree of coherence superposed to the thermal noise. This external forcing is characterized by several high frequency events randomly distributed in space and time. The explicit form is given by:

$$\Psi_{HF} = A_{HF} \sum_{n=1}^N e^{-[(x-x_n)/(h_x(1\pm c_n))]^2} e^{-(t-t_n)/(h_t(1\pm d_n))} \quad (9)$$

where  $A_{HF}$  is a normalization factor such that  $\max(\nabla\Psi_{HF} = 1)$ ,  $N$  is the total number of “events”,  $x_n$  and  $t_n$  the random distributed positions,  $h_x$  and  $h_t$  the characteristic length and timescale and, finally,  $c_n$  and  $d_n$  random numbers between 0

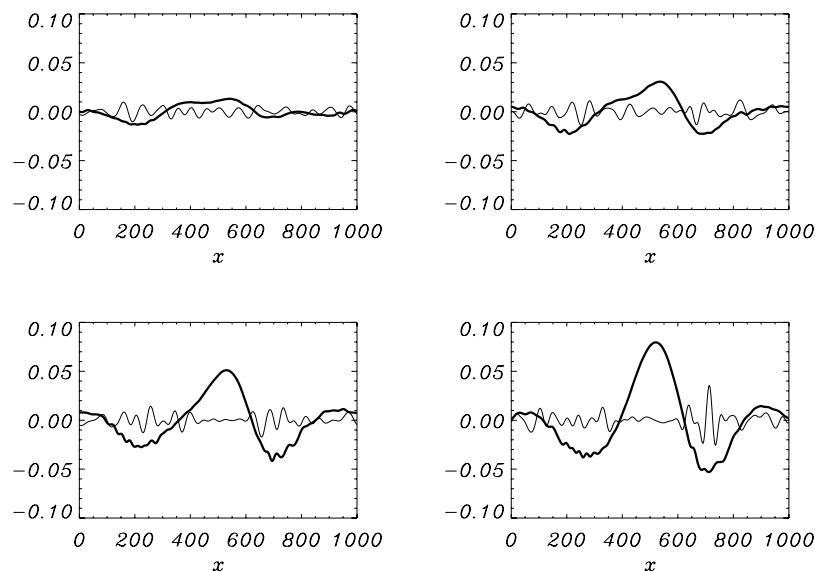


**Figure 4.** Proton fluctuations (thick continuous line) and the charge separation  $\delta q = n_p - n_e$  (continuous line) at  $t = 1500, 2000, 2500, 3000$ .

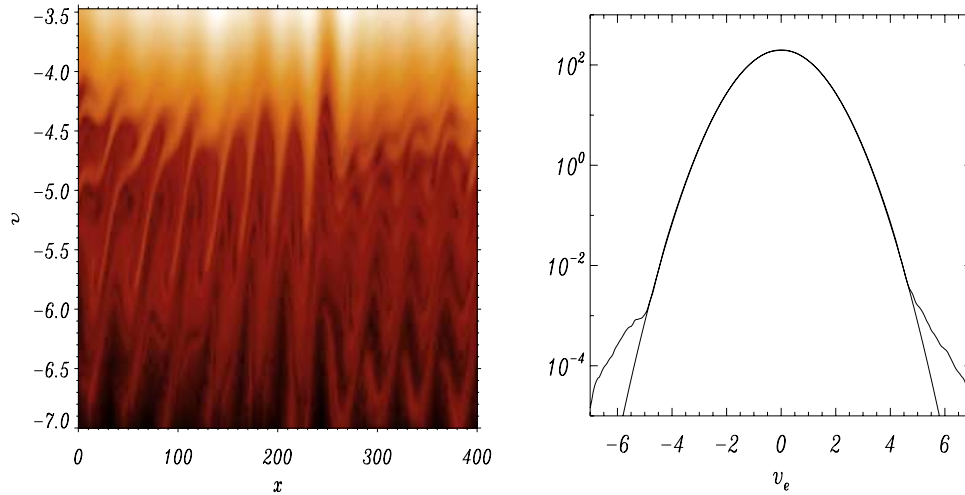


**Figure 5.** (Left) Shaded isocontours of the e.d.f. in the phase space strip  $0 \leq x \leq 400$ ,  $-7 \leq v_e \leq -3.5$  at  $t = 4000$ . (Right) e.d.f. versus  $v_e$  averaged in  $x$  at  $t = 0, 4000$ . The simulation has been performed with  $\eta = 0.03$  and  $\epsilon = 0.03$ .

and 1. We have tried a number of different analytical not Gaussian-like forms for  $\Psi_{HF}$  which show that the global effect of any complicated forcing term can be represented as a sum of plasma pulses. Therefore we have chosen to use the Gaussian profile (for the potential) in order to control the characteristic length scales injected into the system. The parameters of the HF and LF forcing are chosen such to induce electrons fluctuations on a typical length scale of the order of a tenth of Debye lengths, i.e.,  $\lambda_{HF} \sim 20 \lambda_D$ , and protons fluctuations with a typical length scale of the order of hundred of Debye lengths, i.e.,  $\lambda_{LF} \sim 100 \lambda_D$ . A visual representation of the forcing used in the simulations is shown in Figure 2 where we draw the space-time shaded isocontours of the LF and HF forcing in the  $(x, t)$  space for  $1000 \leq t \leq 3500$ .

#### 4. Numerical Results

[31] We integrate the Vlasov-Poisson (with external forcing) system of equations (4)–(6) in the  $(x, v_e, v_p)$  phase space defined by  $x \in [0, L_x]$ ,  $v_e \in [-\hat{v}_e, \hat{v}_e]$ ,  $v_p \in [-\hat{v}_p, \hat{v}_p]$ . We take a spatial interval  $L_x$  of  $10^3 \lambda_D$  and a electron to proton mass ratio  $m_e/m_p = 1/1836$ . The numerical parameters are:  $\hat{v}_e = 8.0$ ,  $\hat{v}_p = 0.2$ ,  $dx = 0.5$ ,  $dv_e = 0.016$ ,  $dv_p = 0.0004$  (here  $dv_e$  and  $dv_p$  represent the velocity space grid length). The forcing parameters are the same as in Figure 2.

[32] We take at the initial time a homogeneous thermal plasma with a single Maxwellian population for both electron and protons with the same temperature. The corresponding initial particle densities and temperatures are normalized to one:

$$\begin{aligned} f_e(x, v_e, t = 0) &= \frac{1}{\sqrt{2\pi}} e^{-v_e^2/2}, \\ f_p(x, v_p, t = 0) &= \frac{1}{\sqrt{2\pi}\mu} e^{-v_p^2/2\mu}, \\ n_e = n_p = 1, \quad T_e = T_p = 1 \end{aligned} \quad (10)$$

where  $\mu = m_e/m_p$ .

[33] We present now the results of a simulation with  $\eta = 0.03$  and  $\epsilon = 0.03$ . In Figure 3 we show the proton density fluctuations,  $\delta n_p$ , and the electric field fluctuations,  $\delta E$ , in the  $(x, t)$  plane. First of all, despite  $K \gg 1$ , the LF forcing generates, for  $t > 2000$ , a central bump with two lateral cavities. The proton density variations are of the order of  $|\delta n_p| \sim 0.05$ , which can be considered as consistent with the typical values observed in the solar wind. In the absence of the HF forcing, the electrons would screen almost completely such density inhomogeneity following the Boltzmann distribution of equation (8) thus almost completely neutralizing any charge separation induced by LF motions. However, plasma oscillations of the order of  $|\delta E| \sim 0.025$  are generated by the HF forcing term and concentrate more and more, in the form of “wave trains”, in the density cavities where they are amplified to larger values,  $|\delta E| \sim 0.2$ , (see the right frame of Figure 3). This process is well outlined in Figure 4 where we plot the proton fluctuations (thick continuous line) and the charge separation  $\delta q = n_p - n_e$  (continuous line) at  $t = 1500, 2000, 2500, 3000$ . We see that the progressive formation of proton inhomogeneities is accompanied by the smoothing of  $\delta q$  in the central bumped region,  $400 < x < 600$ , and by the concentration and amplification of  $\delta q$  in the cavities around  $x_1 \sim 270$  and  $x_2 \sim 700$ . Then, due to the presence of plasma density gradients, the relatively large amplitude plasma oscillations break due to the self-intersection of electron trajectories. As a results, a significant fraction of the electrons are accelerated to larger velocity values (see for example *Bulanov et al. [1990]*). The ejection of the electrons is clearly seen in Figure 5, left frame, where we draw the shaded isocontours of the e.d.f. at  $t = 4000$  in a strip of the phase space,  $0 \leq x \leq 400$ ,  $-7 \leq v_e \leq -3.5$ . We see that the e.d.f. is characterized by elongated finger structures extending toward larger velocity values, a typical signature of the acceleration process. In Figure 5, right frame, we show the  $x$ -averaged e.d.f. versus  $v_e$  at  $t = 0, 4000$ . We see the formation of an halo for velocity values  $v_e > 5$ . According to *Bulanov et al. [1990]*, the characteristic breaking time of plasma oscillations with  $\lambda$  of the order of several Debye lengths in a

plasma with an inhomogeneous scale length  $l_{inh} \sim 100\lambda_D$  (as in our simulation) is of the order of  $t_{wb} \sim 100-1000 \omega_{pe}^{-1}$ . This is consistent with the observed formation time of the halo on the e.d.f. in our simulation.

[34] We have performed many other simulations by varying the amplitude of the LF and HF forcing. The results are summarized as follows.

[35] When the HF forcing is reduced below  $\epsilon = 0.01$ , no significant halo formation is observed since the electric field fluctuations in the density cavities is not sufficiently large to accelerate the electrons even in the presence of the same plasma inhomogeneities. When instead the HF forcing is unchanged,  $\epsilon = 0.03$ , but the proton density gradients are reduced to  $\delta n_p \leq 0.01$  by decreasing the LF forcing, still no halo is observed due to the lack of the interaction of the plasma oscillations with plasma inhomogeneities (in other words,  $t_{wb}$  becomes too large). Furthermore, in the limit where no HF forcing is present,  $\epsilon = 0$ , and for increasing values of the LF forcing, the system generates stronger and stronger density cavities up to  $|\delta n_p| \sim 0.4$  for  $\eta = 0.1$  associated with a low amplitude  $|E^{\max}| \sim 0.005$ , quasi stationary, multipolar electric field. However, even with such a non realistic high proton fluctuation level, no halo is produced at all since the electron response is purely adiabatic, as discussed in section 3.1, and no high frequency motions are generated. Finally, in the limit case of no LF forcing,  $\eta = 0$ , but for a very strong HF forcing,  $\epsilon \geq 0.1$ , we observe the generation of a halo on the e.d.f. Indeed, the plasma oscillations are so strong,  $|E^{\max}| \sim 1$ , that self-generated proton density cavities are produced by ponderomotive effects [Califano and Lontano, 1999] and, in any case, the amplitude of the Langmuir oscillations are so large that wave-breaking occurs even in the limit of a homogeneous plasma. However, such a large level of HF fluctuations seems unrealistic for solar wind applications.

## 5. Conclusions

[36] In this paper we have considered the problem of the self-consistent generation of an electron halo in a weakly collisional plasma. The “collisions” are (roughly) modeled by an external high frequency forcing added to the electron and proton Vlasov equation. A low frequency forcing is added to the proton Vlasov equation only in order to induce quasi-neutral density fluctuations as a background condition reminiscent of solar wind conditions. The results can be summarized as follows.

[37] If the high frequency external forcing is the only source of motions, nothing much happens when this forcing is not too strong, i.e., when the corresponding acceleration during the coherence time is smaller than the thermal velocity, in our unit when  $\epsilon h_i < 1$  (see equation (9)).

[38] On the other hand, adding a low frequency forcing strongly modifies the picture for the same relatively moderate values of the high frequency forcing. We observe that Langmuir wave packets are trapped in the proton density cavities, leading to the generation of suprathermal electrons forming a halo on the distribution function. It is worth to underline that, as soon as the density fluctuations are generated, the halo formation is observed to occur over a time which scales, very roughly, as  $\epsilon^{1/2}$ , in agreement with

the diffusive nature of a “collisional” mechanism. In order to maintain our computations within reasonable time limits, we have taken values of  $\epsilon$  about two order of magnitudes larger than the values obtained from equation (1) using solar wind parameters. However, if we extrapolate the above scaling, we can speculate that the timescale to establish a halo in solar wind conditions will be of the order of a few ten of seconds comparable with the time resolution of the instruments. It is worth to underline that the main ingredient used here to generate suprathermal electron tails is the discrete particle effect modeled, in this work, by the “non Vlasov” high frequency forcing term, a result which is somewhat similar to what was recently found by Yoon *et al.* [2006] and Rhee *et al.* [2006].

[39] The main limit of our calculations is that they are one dimensional. For this reason, we cannot directly compare our results to the solar wind plasma. On the other hand, for typical values of the solar wind magnetic field, the electron gyroperiod is much shorter than the electron collision time. Therefore one can expect that the one dimensional picture of our model is not totally unrealistic. However, this could explain only the formation of a halo population along the magnetic field, i.e., in the sunward and antisunward directions. One may speculate that diffusion by Whistler Waves, as discussed by Saito and Gary [2007], will isotropise the distribution of the halo. This diffusion cannot be fully isotropic since the whistler waves propagate mainly along the magnetic field which may explain the depletions observed at times in the perpendicular direction.

[40] In conclusion, the results we have described are encouraging, but must be only considered as a first step toward a 3D magnetized approach.

[41] **Acknowledgments.** This work was supported, in part, by the Paris VII University, the Paris Observatory and the CNRS. The calculations were performed at the super computing center S.I.O. (Observatoire de Paris).

[42] Amitava Bhattacharjee thanks Chung-Sang Ng and Peter Yoon for their assistance in evaluating this paper.

## References

- Albright, B. J., M. E. Jones, D. S. Lemons, and D. Winske (2001), Kinetic plasma modeling with quiet Monte Carlo direct simulation, in *Proceedings of ISSS-6*, edited by J. Büchner, C. T. Dum, and M. Scholer, p. 214, Copernicus Gesellschaft, Garching, Germany.
- Alexandrov, A. F., L. S. Bogdankevich, and A. A. Rukhadze (1984), *Principles of Plasma Electrodynamics, Springer Series in Electrophysics*, vol. 9, Springer, New York.
- Bulanov, S., L. Kovrizhnykh, and A. Sakharov (1990), Regular mechanisms of electron and ion acceleration, *Phys. Rep.*, *186*, 1, doi:10.1016/0370-1573(90)90002-J.
- Califano, F., and M. Lontano (1999), Vlasov-Poisson simulations of strong wave-plasma interaction in conditions of relevance for radiofrequency plasma heating, *Phys. Rev. Lett.*, *83*, 96.
- Chateau, Y. F., and N. Meyer-Vernet (1991), Electrostatic noise in non-Maxwellian plasmas: Generic properties and “kappa” distributions, *J. Geophys. Res.*, *96*, 5825.
- Christon, S. P., D. J. Williams, D. G. Mitchell, L. Frank, and C. Huang (1989), Spectral characteristics of plasma sheet ion and electron population during undisturbed geomagnetic conditions, *J. Geophys. Res.*, *94*, 13,409.
- Collier, M. R. (1999), Evolution of kappa distributions under velocity space diffusion: A model for the observed relationship between their spectral parameters, *J. Geophys. Res.*, *104*, 28,559.
- Fairfield, D. H., and J. D. Scudder (1985), Polar rain: Solar coronal electrons in the Earth’s magnetosphere, *J. Geophys. Res.*, *90*, 4055.
- Feldman, U., U. Schhhle, K. G. Widing, and J. M. Laming (1998), Coronal composition above the solar equator and the North Pole as determined from spectra acquired by the SUMER instrument on SOHO, *Astrophys. J.*, *505*, 999, doi:10.1086/306195.

- Gosling, J. T. (1999), On the determination of electron polytrope indices within coronal mass ejections in the solar wind, *J. Geophys. Res.*, *104*, 19,851.
- Hammond, C. M., W. C. Feldman, D. J. McComas, J. L. Phillips, and R. J. Forsyth (1996), Variation of electron-strahl width in the high-speed solar wind: Ulysses observations, *Astron. Astrophys.*, *316*, 350–354.
- Hammond, C. M., J. L. Phillips, G. K. Crawford, and A. Balogh (1996), The relationship between electron density and temperature inside coronal mass ejections, in *Solar Wind Eight*, edited by D. Winterhalter et al., pp. 558–561, *AIP Conf. Proc.*, vol. 382.
- Hasegawa, A., K. Mima, and M. Duong-van (1985), Plasma distribution function in a superthermal radiation field, *Phys. Rev. Lett.*, *54*, 2608, doi:10.1103/PhysRevLett.54.2608.
- Jones, M. E., D. S. Lemons, R. J. Mason, V. A. Thomas, and D. Winske (1996), A grid based Coulomb collision model for PIC codes, *J. Comput. Phys.*, *123*, 169.
- Leubner, M. P. (2001), Wave induced synergetic electron acceleration in inhomogeneous solar plasmas, in *IAU Symposium 203*, edited by P. Brekke, B. Fleck, and J. B. Gurman, p. 544, Astronomical Society of the Pacific, Int. Astron. Union.
- Lie-Svendsen, Ø., V. Hansteen, and E. Leer (1997), Kinetic electrons in high-speed solar wind streams: Formation of high-energy tails, *J. Geophys. Res.*, *102*, 4701.
- Lie-Svendsen, Ø., and E. Leer (2000), The electron velocity distributions in the high-speed solar wind: Modeling the effects of protons, *J. Geophys. Res.*, *105*, 35.
- Ma, C. Y., and D. Summers (1999), Formation of power-law energy spectra in space plasmas by stochastic acceleration due to Whistler-mode waves, *Geophys. Res. Lett.*, *25*, 4099.
- Maksimovic, M., V. Pierrard, and P. Riley (1997), Ulysses electron distributions fitted with Kappa functions, *Geophys. Res. Lett.*, *24*, 1151.
- Maksimovic, M., et al. (2005), Radial evolution of the electron distribution functions in the fast solar wind between 0.3 and 1.5 AU, *J. Geophys. Res.*, *110*, A09104, doi:10.1029/2005JA011119.
- Mannheimer, W. M., M. Lampe, and G. Joyce (1997), Langevin representation of Coulomb collisions in PIC simulations, *J. Comput. Phys.*, *138*, 563.
- Meyer-Vernet, N., and C. Perche (1989), Tool kit for antennae and thermal noise near the plasma frequency, *J. Geophys. Res.*, *94*, 2405.
- Ogilvie, K. W., R. Fitzreiter, and M. Desch (2000), Electrons in the low-density solar wind, *J. Geophys. Res.*, *105*, 27,277.
- Olbert, S. (1983), Role of thermal conduction in the acceleration of the solar wind, in *Proceeding of Solar Wind Five*, p. 149, NASA.
- Phillips, J. L., and J. T. Gosling (1990), Radial evolution of solar wind thermal electron distributions due to expansion and collisions, *J. Geophys. Res.*, *95*, 4217.
- Pierrard, V., M. Maksimovic, and J. Lemaire (2001), Self-consistent model of solar wind electrons, *J. Geophys. Res.*, *106*, 29,305.
- Qiang, J., R. D. Ryne, and S. Habib (2000), Self-consistent Langevin simulation of Coulomb collisions in charged particle beams, in *Conference on High Performance Networking and Computing*, IEEE Computer Society, Washington, D. C.
- Rhee, T., C.-M. Ryu, and P. H. Yoon (2006), Self-consistent formation of electron kappa distribution: 2. Further numerical investigation, *J. Geophys. Res.*, *111*, A09107, doi:10.1029/2006JA011682.
- Saito, S., and S. P. Gary (2007), Whistler scattering of suprathermal electrons in the solar wind: Particle-in-cell simulations, *J. Geophys. Res.*, *112*, A06116, doi:10.1029/2006JA012216.
- Scudder, J., and S. Olbert (1979a), A theory of local and global processes which affect solar wind electrons: 1. The origin of typical 1 AU velocity distribution functions - Steady state theory, *J. Geophys. Res.*, *84*, 2755.
- Scudder, J., and S. Olbert (1979b), A theory of local and global processes which affect solar wind electrons: 2. Experimental support, *J. Geophys. Res.*, *84*, 6603.
- Skoug, R. M., W. C. Feldman, J. T. Gosling, D. J. McComas, and C. W. Smith (2000), Solar wind electron characteristics inside and outside coronal mass ejections, *J. Geophys. Res.*, *105*, 23,609.
- Vinas, A., H. K. Wong, and A. Klimas (2000), Generation of electron suprathermal tails in the upper solar atmosphere: Implications for coronal heating, *Astrophys. J.*, *528*, 509, doi:10.1086/308151.
- Vocks, C., and G. Mann (2003), Generation of suprathermal electrons by resonant wave-particle interaction in the solar corona and wind, *Astrophys. J.*, *593*, 1134.
- Yoon, P. H., T. Rhee, and C.-M. Ryu (2006), Self-consistent formation of electron kappa distribution: 1. Theory, *J. Geophys. Res.*, *111*, A09106, doi:10.1029/2006JA011681.

F. Califano, Dipartimento di Fisica, Università di Pisa, Largo Pontecorvo 3, 56127, Pisa, Italy. (califano@df.unipi.it)

A. Mangeney, LESIA, Observatoire de Paris-Meudon, 5 place Jules Janssen, 92195, Meudon Cedex, France. (mangeney@despace.obspm.fr)